Trans. Phenom. Nano Micro Scales, 2(2): 118-131, Summer – Autumn 2014
DOI: 10.7508/tpnms.2014.02.004

ORIGINAL RESEARCH PAPER

Study of Fluid Flow and Heat Transfer of AL_2O_3-Water as a Non-Newtonian Nanofluid through Lid-Driven Enclosure

A.A. Abbasian Arani[1,*], G.A. Sheikhzadeh[1], A. Ghadirian Arani[1]
[1]*Mechanical Engineering Department, University of Kashan, Kashan, I.R. Iran*

ARTICLE INFO.

Article history
Received 29 January 2014
Accepted 26 June 2014

Keywords
Enclosure
Mixed Convection
Nanofluid
Non-Newtonian
Numerical
Shear-Thinning

Abstract

Flow field and heat transfer of a nanofluid, whose non-Newtonian behavior has been demonstrated in the laboratory, in a square enclosure have been numerically modeled and investigated. To estimate the viscosity of nanofluid, experimental data of Hong and Kim, 2012 have been used, and a new model has been proposed. Finally, the obtained results have been compared to those of Newtonian behavior. The results obtained by the numerical simulation indicate that the average Nusselt number with non-Newtonian behavior has a value less than the Newtonian behavior. Also for the case in which the nanofluid is non-Newtonian, the buoyancy force is often insignificant, and forced convection dominates. By adding the nanoparticles, the average Nusselt number for the non-Newtonian nanofluid increases, but for the Newtonian nanofluid, depending on the dominant of natural or forced convection in the flow, it decreases or increases, respectively. On the other hand, with increasing the Reynolds number, the heat transfer rate increases for both Newtonian and non-Newtonian fluid at any constant Grashof number, while with increasing of Grashof number at a given temperature difference and a constant Reynolds number, the heat transfer rate increases and decreases in Newtonian and non-Newtonian nanofluids, respectively.

1. Introduction

Rheological behaviour of nanofluids could be strongly affected by the preparation method of nanofluids [1], viscosity of the base fluid, particles shape and size [2], particles concentration, temperature, surfactant and dispersion state of the nanoparticles [3]. Althoughthe Newtonian fluids has received considerable attention, there are only a limited number of articles dealing with the non- Newtonian fluids. Kwak and Kim [4] have studied experimentally the viscosity of CuO–EG nanofluid. They have found that the viscosities of nanofluid depend on shear thinning and zero shear viscosity increases rapidly when φ exceeds 0.2%. Similar syudy were done by Chang et al. [5] with CuO–water nanofluid, by Ding et al. [6] with CNT–water nanofluid, Aladag et al. [3]and Hong and Kim [7] with Al_2O_3-water nanofluid. Recently Putra et al. [8], Wen and Ding [9] and Santra et al. [10] have numerically investigated the heat transfer in a differentially heated square cavity considering non-Newtonian power law model.

[*]Corresponding author
Email address: abbasian@kashanu.ac.ir

Nomenclature

c_p	specific heat, J/(kg K)	φ	solid volume fraction
Gr	Grashof number	α	thermal diffusivity
D	diameter of nanoparticles	ρ	Density
g	gravitational acceleration, m/s^2	μ	dynamic viscosity
h	heat transfer coefficient, W/(m^2 K)	μ_0	Newtonian plateau
k	thermal conductivity, W/(mK)	μ_∞	Newtonian plateau
kb	Boltzman constant, (JK^{-1}), 1.38066×10^{-23}	υ	kinematics viscosity
L	enclosure length, m	θ	dimensionless temperature
m,K	Flow consistency index	τ	Shear stress
Nu	Nusselt number	γ	Shear rate
p	pressure, N/m^2	ψ	Stream function
P	Dimensionless presure		**Subscripts**
Pr	Prandtle number	avg	Average
Ri	Richardson number	c	cold wall
T	Temperature, K	eff	Effective
u,v	velocity components, m/s	f	Fluid
U,V	dimensionless velocity components	h	hot wall
x,y	Cartesian coordinates, m	nf	Nanofluid
X,Y	dimensionless Cartesian coordinates	p	Particles
	Greek Symbols	s	Solid
β	thermal expansion coefficient	n	Flow behavior index

Power low model for non-Newtonian fluid defined as Equation 1, in order to find out a correlation between shear stress and shear rate:

$$\tau = m\dot{\gamma}^n \tag{1}$$

where τ is the shear stress in Pa, *n* is the flow behavior index, *m* is the flow consistency index in Pa.s^n and γ is the shear rate in s^{-1}.

In order to rectify some of the weaknesses of the power-law, Cross [11] presented the following empirical form which has gained wide acceptance in the literature. In simple shear, it is written as:

$$\frac{\mu-\mu_\infty}{\mu_0-\mu_\infty} = \frac{1}{1+(K\dot{\gamma})^n} \tag{2}$$

In Equation 2, μ_0 is the zero shear viscosity or lower Newtonian plateau in the limit of $\gamma \to 0$ and μ_∞ is the upper Newtonian plateau in the limit of $\gamma \to \infty$. A simple but versatile model that can cope with a yield stress,yet retain the proper extreme of a finite zero and infinite shear-rate viscosity is the Cross model with the exponent set to unity, so:

$$\frac{\mu-\mu_\infty}{\mu_0-\mu_\infty} = \frac{1}{1+(K\dot{\gamma})} \tag{3}$$

Ozoe and Churchill [12] aimed to determining numerically the threshold for the onset of Rayleigh-Benard convection in power law fluids. Kim et al. [13] considered transient buoyant convection in a square cavity subjected to hot and cold temperature on the vertical side walls for Newtonian and non-Newtonian shear-thinning power law fluids of the Ostwald-De Waele type.

Mixed convection Newtonian and non-Newtonian flows in a lid-driven cavity are encountered in a variety of thermal engineering applications including cooling of electronic devices, lubrication technologies, high-performance building insulation, multi-shield structures used for nuclear reactors, food processing, glass production, solar power collectors, drying technologies and others [14]. Numerous studies on lid-driven cavity flow and heat transfer involving different cavity configurations, various fluids and imposed temperature gradients have been continually published in the literature [15-25]. All of the previous studies used a pure base fluid. On the other hand, Tiwari and Das [26] and Muthtamilselvan et al. [27] investigated numerically heat transfer augmentation in a lid-driven cavity filled with a nanofluid and found

that the presence of nanoparticles in a base fluid is capable of increasing the heat transfer capacity of the base fluid.

What is common in most of the above referenced work on nanofluid natural and mixed convection problems is the use of the Brinkman viscosity model [28] for a nanofluid and therefore, predict enhancement of heat transfer due to the presence of nanoparticles. However, there appear some inconsistent findings concerning the convection characteristics of nanofluids. One can relate this incosistency to Newtonian or non-Newtonian assumption in viscosity prediction. Based on refered idea, the objective of this work is a study on flow field and heat transfer characteristics of nanofluid with non-Newtonian assumption for viscosity.

It is worth to say that it is a number of work for convection heat transfer for non-Newtonian fluid/nanofluid in liturature [29-31], but one cannot find any work that was done in cavity.

The viscosity of Alumina/water nanofluids initially decreases with increasing the shear rate; this indicates that the behavior of nanofluid is non-Newtonian shear-thinning [7]. In this study, flow field and heat transfer of Al_2O_3-water nanofluid on lid-driven enclosure with a non-Newtonian behavior based on empirical works have been studied.

2. Mathematical formulation

2.1. Problem Statement

The geometry of the present problem is shown in Figure 1. It consists of a two-dimensional square enclosure of height H and width L. For the present case, we consider H = L.

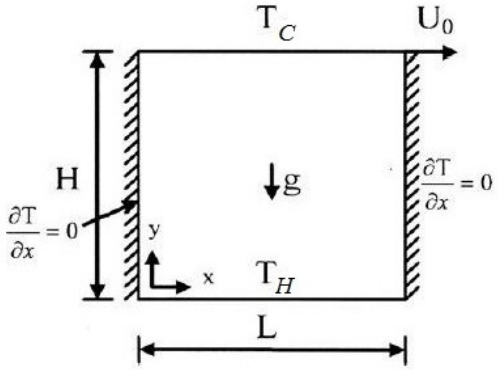


Fig. 1. A schematic view of the cavity with boundary conditions considered in the present study.

The sidewalls of the cavity have been considered to be insulated i.e., non-conducting and impermeable to mass transfer. The temperatures of the top and the bottom horizontal walls are maintained at T_C and T_H, where T_C has been considered as the reference condition. The enclosure is filled with a mixture of water and solid spherical Al_2O_3 particles of 50 nm diameter. The nanoparticles are of uniform shape and size. The nanofluid is assumed to be non-Newtonian, incompressible and the flow is laminar. Also it is assumed that the liquid and solid are in thermal equilibrium and they flow at same velocity. The density varies only in buoyant force, body which has been incorporated only in the body force term by employing the Boussinesq approximation**.**

2.2. Governing equations and boundary conditions

The continuity, momentum and energy equations for a steady, two-dimensional flow of a Fourier constant property fluid have been considered. The governing equations for a steady, two-dimensional flow are as follows:

$$\frac{\partial u}{\partial x}+\frac{\partial v}{\partial y}=0 \tag{4}$$

$$\rho_{nf,0}\left(u\frac{\partial u}{\partial x}+v\frac{\partial u}{\partial y}\right)=-\frac{\partial p}{\partial x}+\frac{\partial \tau_{xx}}{\partial x}+\frac{\partial \tau_{xy}}{\partial y} \tag{5}$$

$$\rho_{nf,0}\left(u\frac{\partial v}{\partial x}+v\frac{\partial v}{\partial y}\right)=-\frac{\partial p}{\partial y}+\frac{\partial \tau_{yx}}{\partial x}+\frac{\partial \tau_{yy}}{\partial y}+(\rho\beta)_{nf,0}g\left(T-T_C\right) \tag{6}$$

$$\rho_{nf,0}\left(u\frac{\partial T}{\partial x}+v\frac{\partial T}{\partial y}\right)=\frac{k_{nf,0}}{c_{pnf,0}}\left(\frac{\partial^2 T}{\partial x^2}+\frac{\partial^2 T}{\partial y^2}\right) \tag{7}$$

For an incompressible Newtonian fluid the relationships between the shear stress and shear rate in case of two-dimensional motion in rectangular coordinate are as follows [32]:

$$\tau_{xx}=\mu_{nf}\left(\frac{\partial u}{\partial x}\right) \tag{8}$$

$$\tau_{xy}=\tau_{yx}=\frac{1}{2}\mu_{nf}\left(\frac{\partial u}{\partial y}+\frac{\partial v}{\partial x}\right) \tag{9}$$

$$\tau_{yy}=\mu_{nf}\left(\frac{\partial v}{\partial y}\right) \tag{10}$$

Where the effective dynamic viscosity of the nano

fluid as given by Khanafer and Vafai [33] is as follows:

$$\mu_{eff} = -0.4491 + \frac{28.837}{T} + 0.574\varphi_p - 0.1634\varphi_p^2 + 23.053\frac{\varphi_p^2}{T^2} + 0.0132\varphi_p^3 - 2354.735\frac{\varphi_p}{T^3} + 23.498\frac{\varphi_p^2}{d_p^2} - 3.0185\frac{\varphi_p^3}{d_p^2} \quad (11)$$

Where Φ_p and d_p are solid volume fraction and solid particle diameter respectively.

For a non-Newtonian fluid the relationships between the shear stress and shear rate in case of two-dimensional motion in rectangular co-ordinate according to the Cross model are as follows [11] :

$$\tau_{xy} = \left(\frac{\mu_0 - \mu_\infty}{1 + K\left|\sqrt{\frac{1}{2}(\dot{\gamma}.\dot{\gamma})}\right|} + \mu_\infty \right)\dot{\gamma} \quad (12)$$

Where:

$$\frac{1}{2}(\dot{\gamma}.\dot{\gamma}) = 2\left(\left(\frac{\partial u}{\partial x}\right)^2 + \left(\frac{\partial v}{\partial y}\right)^2\right) + \left(\frac{\partial v}{\partial x} + \frac{\partial u}{\partial y}\right)^2 \quad (13)$$

thus the stress tensors of Equations 2 and 3 take the following forms:

$$\tau_{xx} = 2\left(\frac{\mu_0 - \mu_\infty}{1 + K\left(2\left(\left(\frac{\partial u}{\partial x}\right)^2 + \left(\frac{\partial v}{\partial y}\right)^2\right) + \left(\frac{\partial v}{\partial x} + \frac{\partial u}{\partial y}\right)^2\right)^{\frac{1}{2}}} + \mu_\infty\right)\left(\frac{\partial u}{\partial x}\right) \quad (14)$$

Here K is an empirical constant, which depend on the type of used nanofluid. Hong and Kim [7] have shown experimentally the relation between the shear stress and shear strain for Al_2O_3–water nanofluid.

Using this data, the values of K has been calculated for 1%, 3% and 5% solid volume fraction. The values of K for different φ have been given in Table 1. It is to be noted that Newtonian limit is recovered here when K → 0 [34].

$$\tau_{xy} = \tau_{yx} = \left(\frac{\mu_0 - \mu_\infty}{1 + K\left(2\left(\left(\frac{\partial u}{\partial x}\right)^2 + \left(\frac{\partial v}{\partial y}\right)^2\right) + \left(\frac{\partial v}{\partial x} + \frac{\partial u}{\partial y}\right)^2\right)^{\frac{1}{2}}} + \mu_\infty\right)\left(\frac{\partial u}{\partial y} + \frac{\partial v}{\partial x}\right) \quad (15)$$

$$\tau_{yy} = 2\left(\frac{\mu_0 - \mu_\infty}{1 + K\left(2\left(\left(\frac{\partial u}{\partial x}\right)^2 + \left(\frac{\partial v}{\partial y}\right)^2\right) + \left(\frac{\partial v}{\partial x} + \frac{\partial u}{\partial y}\right)^2\right)^{\frac{1}{2}}} + \mu_\infty\right)\left(\frac{\partial v}{\partial y}\right) \quad (16)$$

The effective density of the nanofluid at reference temperature is:

$$\rho_{nf} = (1-\phi)\rho_{f,0} + \phi\rho_{p,0} \quad (17)$$

and the heat capacitance of nanofluid is:

$$(\rho c_p)_{nf} = (1-\phi)(\rho c_p)_{f,0} + \phi(\rho c_p)_{p,0} \quad (18)$$

as given by Xuan et al. [35].

The effective thermal conductivity of fluid has been determined by the model proposed by Patel et al. [36]. For the two component entity of spherical-particle suspension the model gives:

$$\frac{k_{eff}}{k_f} = 1 + \frac{k_p A_p}{k_f A_f} + ck_p Pe\frac{A_p}{k_f A_f} \quad (19)$$

Where

$$\frac{A_p}{A_f} = \frac{d_f}{d_p}\frac{\phi}{(1-\phi)} \quad (20)$$

In above equations k and d referd to thermal conductivity and particle diamete respectivily. In addition p and f refers to solid nano particles and fluid as indices respectivily. In Equation 19 c is a cosctant. and Pe= $u_p d_p / \alpha_f$, where u_p is the Brownian motion velocity of the particles which is given by:

$$u_p = \left(2k_b T\right)/\left(\pi\mu_f {d_p}^2\right) \quad (21)$$

Table 1
Values of fluid behaviour index parameters

Φ	$\mu_0(p_{a.s})$	$\mu_\infty(p_{a.s})$	K(s)
0.01	61.655	0.005	220.1
0.03	150.011	0.011	706.3
0.05	208.231	0.031	1005.0

In above equation k_b is Boltzmann's constant (1.38066×10^{-23} J/K). The calculation of effective thermal conductivity can be obtained from Equation 19. The governing equations (4-7) can be converted to non-dimensional form, using the following dimensionless parameters:

$$(X,Y)=(x,y)/H,\quad (U,V)=(u,v)/U_0 \tag{22}$$

$$P=p/\rho_{f,0}U_0^{\,2},\qquad \theta=(T-T_C)/(T_H-T_C) \tag{23}$$

Then the non-dimensional equations will be as follows

$$\frac{\partial U}{\partial X}+\frac{\partial V}{\partial Y}=0 \tag{24}$$

$$\rho^*\left(U\frac{\partial U}{\partial X}+V\frac{\partial U}{\partial Y}\right)=-\frac{\partial P}{\partial X}+\frac{1}{\mathrm{Re}}\left(\frac{\partial}{\partial X}\left(\mu^*\frac{\partial U}{\partial X}\right)+\frac{\partial}{\partial Y}\left(\mu^*\frac{\partial U}{\partial Y}\right)\right) \tag{25}$$

$$\rho^*\left(U\frac{\partial V}{\partial X}+V\frac{\partial V}{\partial Y}\right)=-\frac{\partial P}{\partial Y}+\frac{1}{\mathrm{Re}}\left(\frac{\partial}{\partial X}\left(\mu^*\frac{\partial V}{\partial X}\right)+\frac{\partial}{\partial Y}\left(\mu^*\frac{\partial V}{\partial Y}\right)\right)+Ri.\rho^*.\beta^*.\theta \tag{26}$$

$$\rho^*(U\frac{\partial\theta}{\partial X}+V\frac{\partial\theta}{\partial Y})=\frac{1}{\mathrm{Re}\,\mathrm{Pr}}\frac{1}{c_p^*}\left(\frac{\partial}{\partial X}\left(k^*\frac{\partial\theta}{\partial X}\right)+\frac{\partial}{\partial Y}\left(k^*\frac{\partial\theta}{\partial Y}\right)\right) \tag{27}$$

Here the apparent viscosity of the nanofluid is:

$$\mu_{app}=\left(\frac{\mu_0-\mu_\infty}{1+k\left(\frac{U_0}{H}\right)L^{\frac{1}{2}}}+\mu_\infty\right) \tag{28}$$

$$L=\left(2\left\{\left(\frac{\partial U}{\partial X}\right)^2+\left(\frac{\partial V}{\partial Y}\right)^2\right\}+\left(\frac{\partial V}{\partial X}+\frac{\partial U}{\partial Y}\right)^2\right)$$

The boundary conditions, used to solve Equations 25 to 27 are as follows.

$$Y=0,0\le X\le1\rightarrow U=V=0,\theta=1 \tag{29}$$

$$Y=1,0\le X\le1\rightarrow U=1,V=\theta=0 \tag{30}$$

$$X=0,0\le Y\le1\rightarrow U=V=\frac{\partial\theta}{\partial X}=0 \tag{31}$$

$$X=1,0\le Y\le1\rightarrow U=V=\frac{\partial\theta}{\partial X}=0 \tag{32}$$

Equations 24 to 27, along with the boundary conditions are solved numerically. From the converged solutions, we have calculated Nu(X) (local Nusselt number) and Nu_b (average Nusselt number) for the bottom hot wall as follows:

$$Nu(X)=-\frac{k_{eff}}{k_f}\frac{\partial\theta}{\partial X}\bigg|_{Y=0,X} \tag{33}$$

$$Nu_b=\overline{Nu}=\int_0^1 Nu(X)\,dX\big|_{Y=0} \tag{34}$$

The dimensionless stream function ψ has been defined as $U=\frac{\partial\psi}{\partial Y}$ and $V=-\frac{\partial\psi}{\partial X}$ the stream function at any grid location *(X, Y)* is calculated as:

$$\psi(X,Y)=\int_{Y_0}^{Y}U.\partial Y+\psi(X,Y_0) \tag{35}$$

Along the solid boundary the stream function is taken as zero. $\psi(X,Y_0)$ is known either from the previous calculation, or, from the boundary condition.

2.3. Numerical approach and validation

The governing mass, momentum and energy equations has been discretized by a control volume approach using a hybrid scheme. The computational domain has been divided into 121 × 121 non-uniform grids. Finer grids have been taken at the boundaries. The set of discretized equations have been solved iteratively, through alternate direction implicit ADI, using the SIMPLER algorithm [37]. For convergence, under-relaxation technique has been employed. To check the convergence, the mass residue of each control volume has been calculated and the maximum value has been used to check the convergence. The convergence criterion has been set to 10^{-6}.

The results are validated with the results of Santra et al. [10] for different *Ra*, which has been summarized in Table 2. The difference between the average Nusselt number of Santra et al. [10] and that

obtained by the present code is well within acceptable limit.

Table 2
Comparison of results for validation

Rayleigh number	Nu of Santra et al. [10]	Nu of present code
1.75	1.75	104
3.87	3.88	105
7.86	7.91	106
1.75	1.75	104

3. Results and discussion

The flow and heat transfer for a range of *Re* and φ have been studied. Water has been considered as the base fluid with $Pr = 6.1$ (considering base temperature as 25°C) [7,38], for present study. Solid spherical Al_2O_3 nanoparticles of 50 nm diameter dispersed in water has been considered as nanofluid.

The temperature dependent effective thermal conductivity of nanofluid has been calculated using the correlation given by Ref. [38]. The physical and thermal properties of both the solid and the fluid at the base temperature i.e. at 25°C have been summarized in Table 3 [7, 38]. The constants μ_0, μ_∞ and K for calculating the shear stresses have been taken from the experimental observation [7].

Table 3
Thermo physical properties of different phase at 25°C

Property	Fluid (water)	Solid (Al_2O_3)
c_p(Jkg-1K-1)	4179	765
ρ (kgm-3)	997.1	3970
k (Wm-1K-1)	0.61	33
β (K-1)	$21.0*10^{-5}$	$0.85*10^{-5}$

Results are presented for $Gr = 10^4$ to 10^6 and Re = 10, 100, 1000 and 2000, while φ has been varied from 0.0% to 5.0%. The hot wall temperature has been considered as 303 K (30°C) while the cold wall temperature is 293 K (20°C).

Since, the heat transfer is strongly affected by the nature of flow; the flow structure has been discussed before presenting the variation of Nusselt number with different parameters.

3.1. Effect of Reynolds number on vertical velocity and temperature

Figures 2a and 2b illustrate the effects of *Re* number on the vertical velocities, for both Newtonian and non-Newtonian behavior respectively, for the water-Al_2O_3 nanofluid and $Gr = 10^4$ at the midsection of the enclosure.

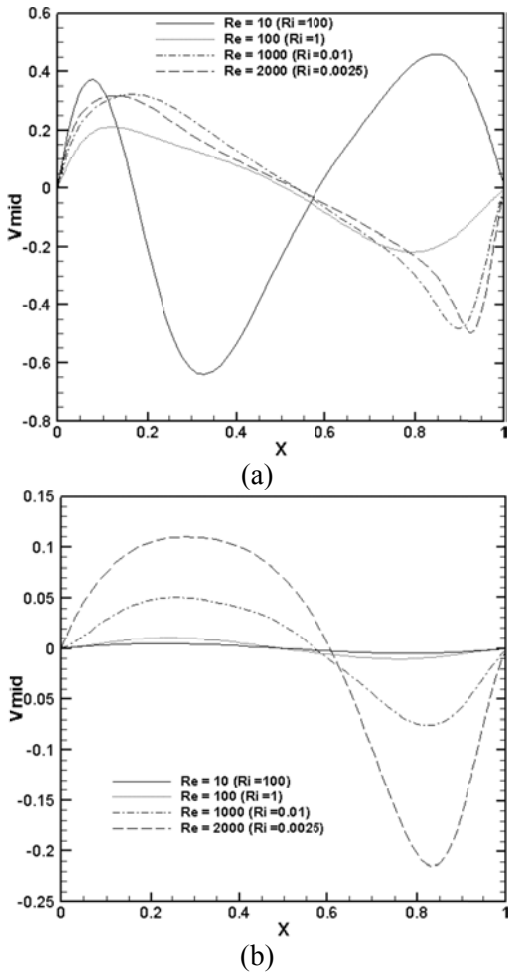


Fig.2. Vertical velocity profile at mid plane for different: a) φ values and $Gr=10^4$ (Newtonian nanofluid) b)Re values and$Gr = 10^4$ (non-Newtonian nanofluid).

There is a significant difference for the velocity profiles between the Re=10 and the others *Re* numbers in Newtonian behavior. This difference is related to the two circulation cells within the enclosure formed only at Re=10 (Figure 3). In general, when the *Re* number is higher, the velocities are smaller at the center of the enclosure than near the walls. Moreover, in non-Newtonian behavior the increase in *Re* number, the value of maximum velocity increases. It seems that, as *Re* number increases, as a result of the effect of moving lid,, for Newtonian and non-Newtonian, nanofluid circulate with higher velocity.

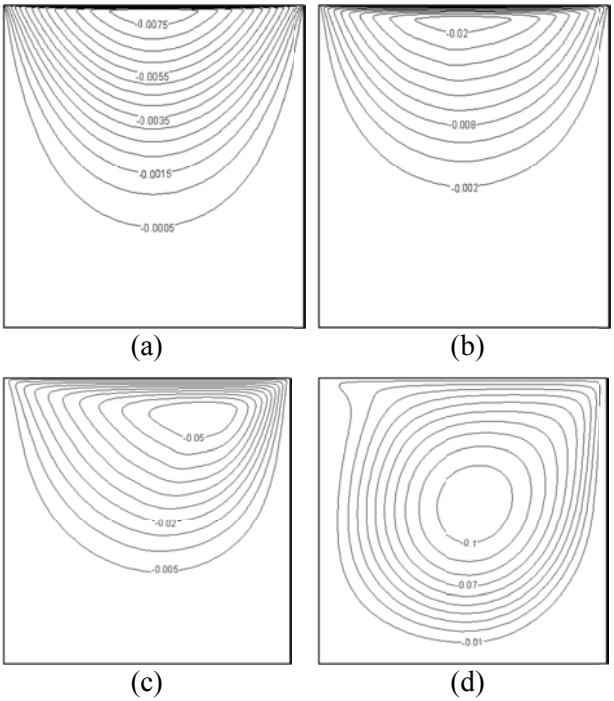


Fig. 3. Streamlines for non- Newtonian behavior, φ= 1.0%, $Gr = 10^4$ and for (a) Re = 10, (b) Re = 100 , (c) Re = 1000 and (d) Re = 2000.

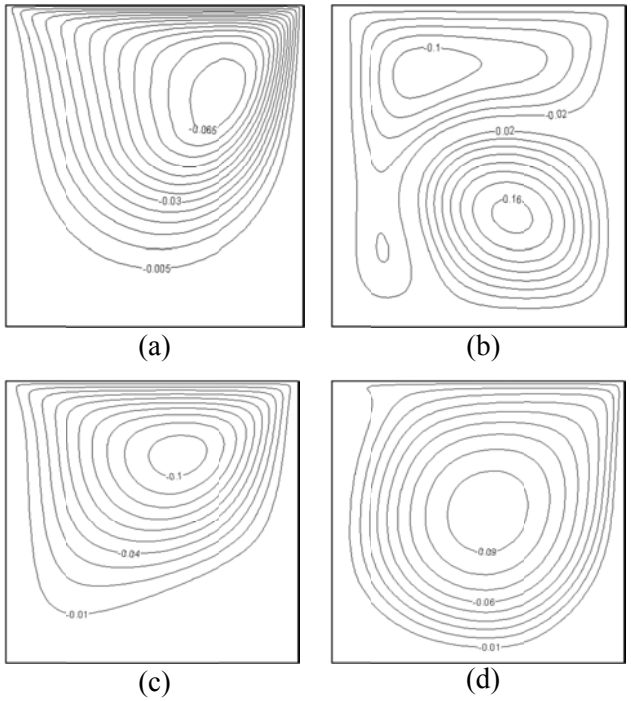


Fig. 4. Streamlines for Newtonian behavior, φ = 1.0%, $Gr = 10^4$ and for (a) Re = 10, (b) Re = 100, (c) Re = 1000 and (d) Re = 2000.

3.2. Effect of non-Newtonian behavior on streamlines and isotherms

Two-dimensional mixed convection is studied for an Al_2O_3–water nanofluid in a square lid-driven cavity for Gr=10^4–10^6, Re=10–2000 and solid volume fraction from 0 to 0.05. Figures 3 and 4 illustrate the stream lines at Re=10-2000 and Gr=10^4 for a non-Newtonian and Newtonian nanofluid with φ=1% respectively. Figure 3a demonstrates that natural convection flow dominates for Re=10. This effect is related to the two circulation cells within the enclosure formed only at Re=10. As the value of Re number increases, the intensity of lid moving effect and hence the intensity of forced convection within the cavity increases as shown in Figures 3b-3d. As can be seen from Figures 3b-3d, the Re number have not effect on the flow field. This phenomenon may be due to increasing cold region and increase of viscosity, but the flow pattern being drawn into the top right corner of cavity.

As the value of Re number increases to 10^5 and 10^6, the intensity of buoyancy and hence the intensity of natural convection within the cavity decreases as shown in Figures 5 and 7 for non-Newtonian behavior and in Figures 6 and 8 for Newtonian behavior with φ=1%.

Increase in Re number augments the effect of lid-driven and hence forced convection flow. But it gradually vanishes with increase in the value of Grashof number, so that at Gr=10^6 the natural convection becomes dominant mode as can be found from comparison between Figures 8a, b and c. For smaller Grashof number, the motion of the upper lid stretches the stream lines towards the right vertical wall and it causes to produce an asymmetric flow pattern.

The isotherms show that for a particular Gr the isotherms shift towards bottom of the cavity as Re number increases. This means that, the term $\partial\theta/\partial Y$ at particular X increases rapidly as Re number increases.

At Ri = 0.01 and 0.1, streamlines show that the forced convection plays a dominant role and the thermal boundary layer forms at the vicinity of horizontal walls. As illustrated in isotherm plots, Figures 9-11, the large core region of the cavity has the same temperature. Due to moving the fluid with the lid, a relative vacuum zone occurred at the left top corner, and then, streamlines deviated from this region. According to Figures 9-11, at Ri = 10 and 100, natural convection is much more effective than forced convection. For the isotherms, it is observed that the thermal boundary layer thickness for non-Newtonian nanofluid is significantly more than that of Newtonian nanofluid.Thus the term $\partial\theta/\partial Y$ is more for Newtonian behavior than non-Newtonian behavior. Since

effective thermal conductivity remains same for both the cases, heat transfer is slightly higher for Newtonian behavior. But the difference is very small. This may be due to the shear thinning nature of nanofluid where effective viscosity becomes almost constant at high shear rate [39]. This feature is common for any Reynolds number. It may be noted that at higher *Re* number, any shear thinning fluid behaves like Newtonian fluid and the thermal boundary layer should be same for both cases. This discrepancy may be due to choosing of models, because actual behavior of viscosity of Al_2O_3–water nanofluid is still unknown.

3.3. Effect of non-Newtonian behavior on viscosity and shear rate field

Figures 12 and 13 illustrate qualitatively the shear rate and viscosity field respectively for Al_2O_3–water nanofluid in non-Newtonian behavior for different *Re* number. Because of high velocity gradient near moving lid, this region has maximum shear rate and far from it shear rate decrease and finally in two bottom corner of enclosure, flow is almost stationary. With increasing of *Re* number, the region near top lid is developed. As discussed in Ref. [7] the viscosities of the nanofluids at low shear rates, decreased gradually as the shear rate increased, indicative of shear thinning behavior. So viscosity close to top lid is low, but far from the lid, the viscosity of the fluid is added.

3.4. Effect of solid volume fraction on average Nusselt number

The variation of the average Nusselt number (*Nu)* along the bottom wall (hot wall) has been presented in Figures 14 and 15 for different *Re* numbers and φ for both Newtonian and non-Newtonian nanofluids. In Newtonian behavior the average Nusselt number *(Nu)* shows a steady decrease in *Nu* with increase in φ, for low *Ri (Ri<1.0)* and increases for high *Ri* (Figure 15).

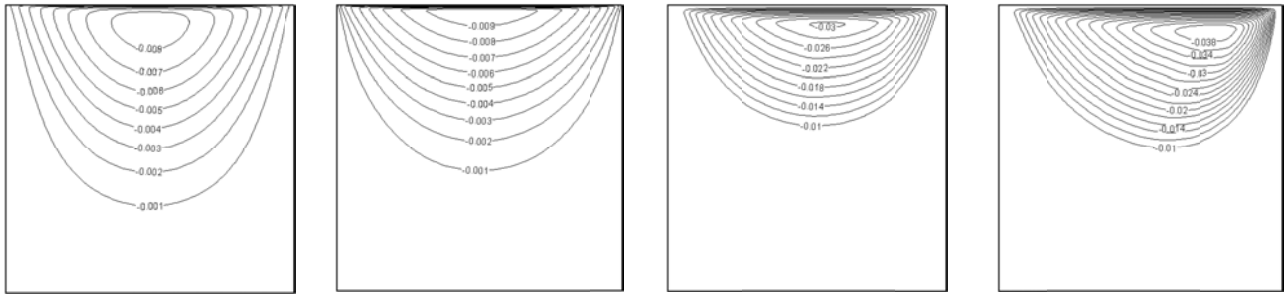
With increase of *Gr* transient from natural convection dominant to forced convection take place at higher *Re* number, but with increase *Re* number at any *Gr* and for a particular φ heat transfer increase. For non-Newtonian behavior Figure 14 shows that *Nu* increases with increase in *Re* number as well as φ. This is due to the increase in effective thermal conductivity of the nanofluid with increase in φ as well as increase in convection heat transfer with the increase in *Re* number. This is contrary to the results obtained in case of Newtonian behavior. As viscosity decreases rapidly with increase in *shear rate*, particularly at non-Newtonian behavior, the effect of buoyancy decreases, which decrease the convective heat transfer rapidly and the increase in velocity of lid is sufficient to cover the loss.

3. Conclusion

Heat transfer enhancement using Al_2O_3–water nanofluid in a two dimensional enclosure has been studied numerically for a range of *Gr* number from 10^4 to 10^6, with a wide range of solid volume fraction ($5.0 \geq \varphi\ (\%) \geq 0.0$). The diameter of Al_2O_3 nanoparticle is 50 nm and Prandtl number of base fluid is 6.1. The numerical analysis has been performed using primitive variables.The fluid has been considered as non-Newtonian in nature.Cross model for a non-Newtonian shear thinning fluid has been selected to calculate shear stresses.

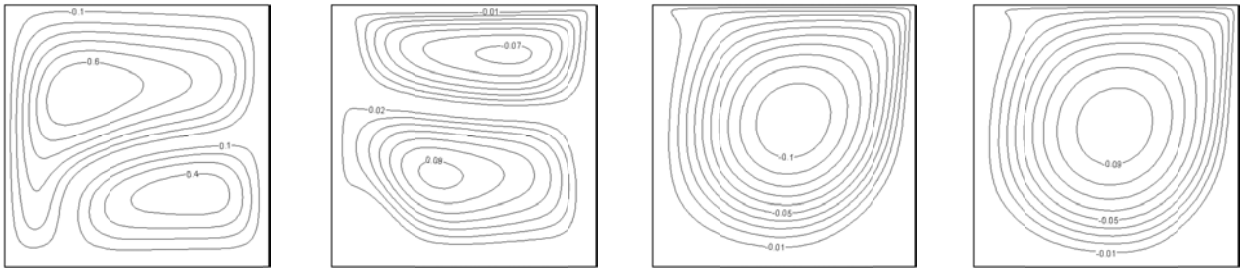
The constants for selected model have been taken from the experiment data of Hong and Kim [7]. The effective thermal conductivity of the nanofluids has been predicted using the model proposed by Patel et al. [36]. The results show increase in heat transfer for increase in solid volume fraction at any Reynolds number. However a considerable decrease in *Nu* number at non-Newtonian behavior is visible than Newtonian behavior.

More experimental investigation needs to be carried out in order to find the actual values of μ_0, μ_∞ and *K* for this kind of nanofluid and actual heat transfer in this kind of geometrical configuration and wide temperature range.



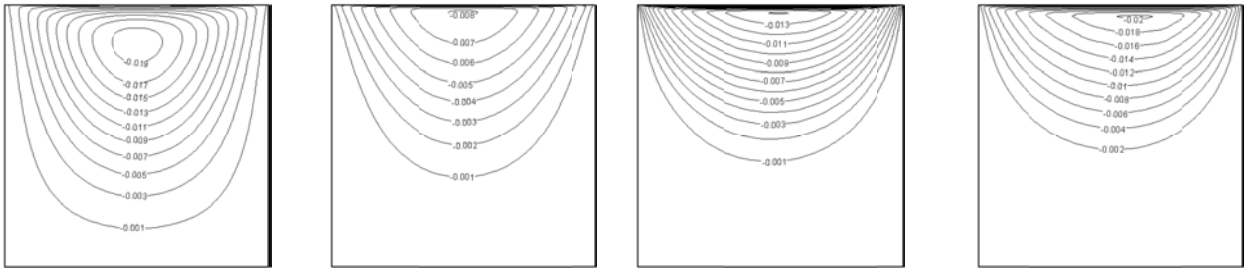
(a) (b) (c) (d)

Fig. 5. Streamlines for non- Newtonian behavior, φ = 1.0%, $Gr = 10^5$ and for (a) Re = 10, (b) Re = 100 , (c) Re = 1000 and (d) Re = 2000.



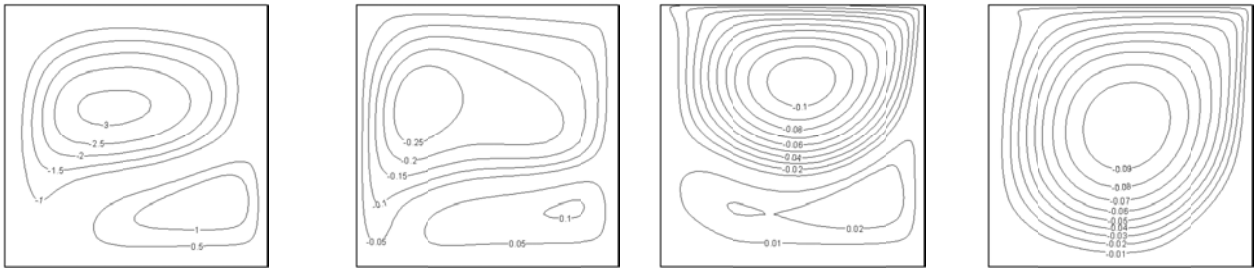
(a) (b) (c) (d)

Fig. 6. Streamlines for Newtonian behavior, φ = 1.0%, $Gr = 10^5$ and for (a) Re = 10, (b) Re = 100, (c) Re = 1000 and (d) Re = 2000.



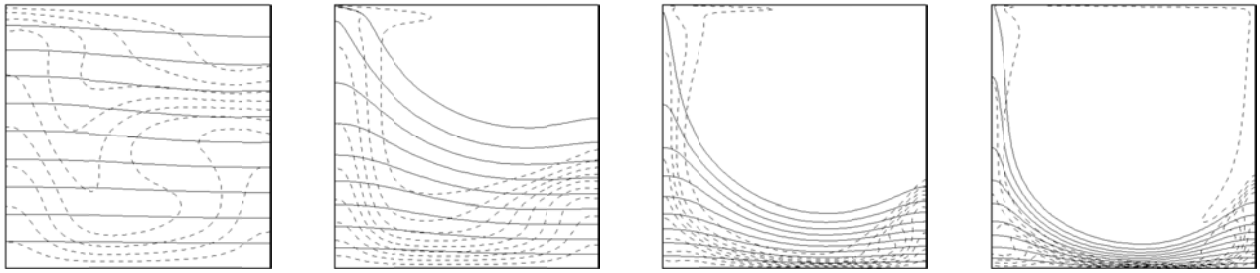
(a) (b) (c) (d)

Fig. 7. Streamlines for non- Newtonian behavior, φ = 1.0%, $Gr = 10^6$ and for (a) Re = 10, (b) Re = 100 , (c) Re = 1000 and (d) Re = 2000.



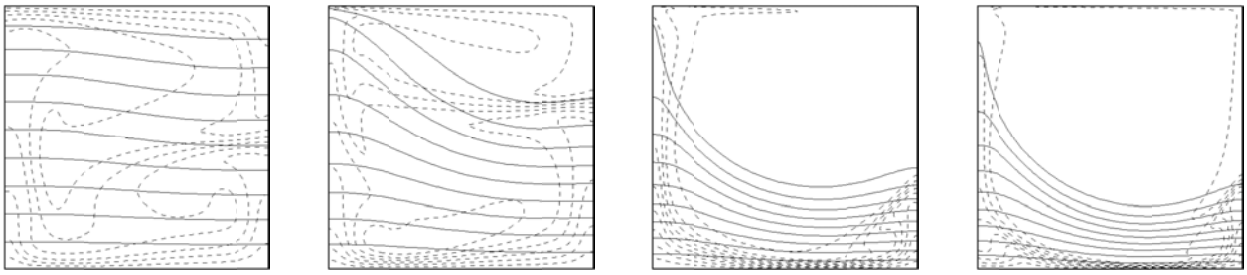
(a) (b) (c) (d)

Fig. 8. Streamlines for Newtonian behavior, φ = 1.0%, $Gr = 10^6$ and for (a) Re = 10, (b) Re = 100, (c) Re = 1000 and (d) Re = 2000.



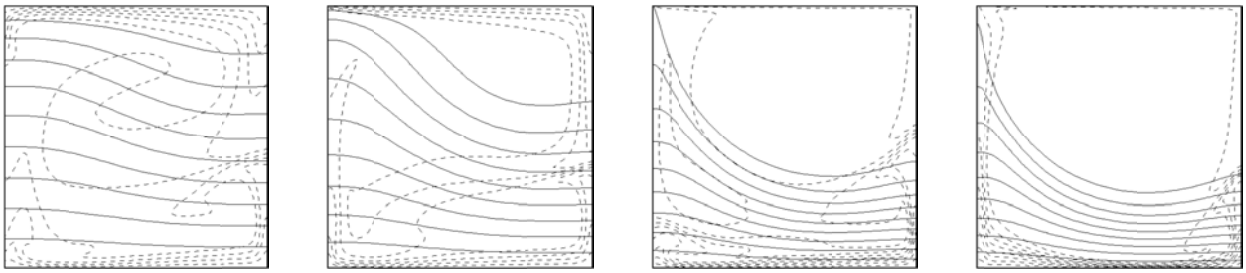
(a) (b) (c) (d)

Fig. 9. Isotherms for φ = 1.0% , for Gr=10^4 and for (a) Re = 10, (b) Re = 100 , (c) Re = 100 and (d) Re = 2000.



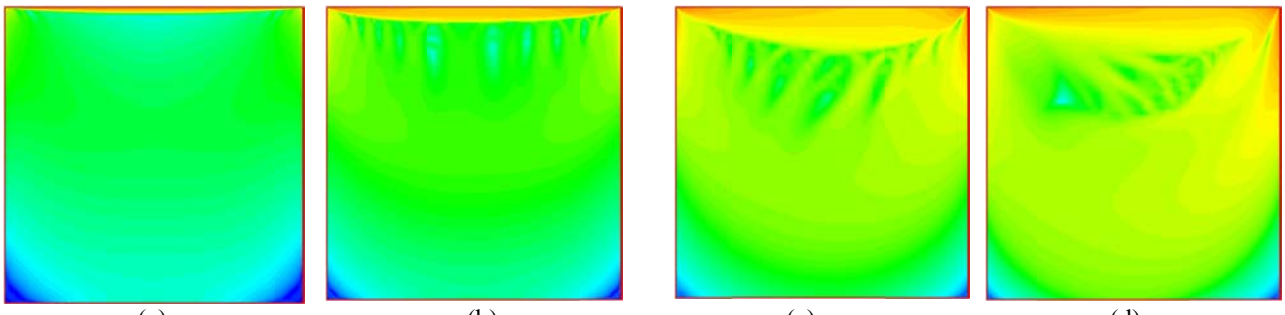
(a) (b) (c) (d)

Fig. 10. Isotherms for φ = 1.0% , for Gr=10^5 and for (a) Re = 10, (b) Re = 100 , (c) Re = 100 and (d) Re = 2000.



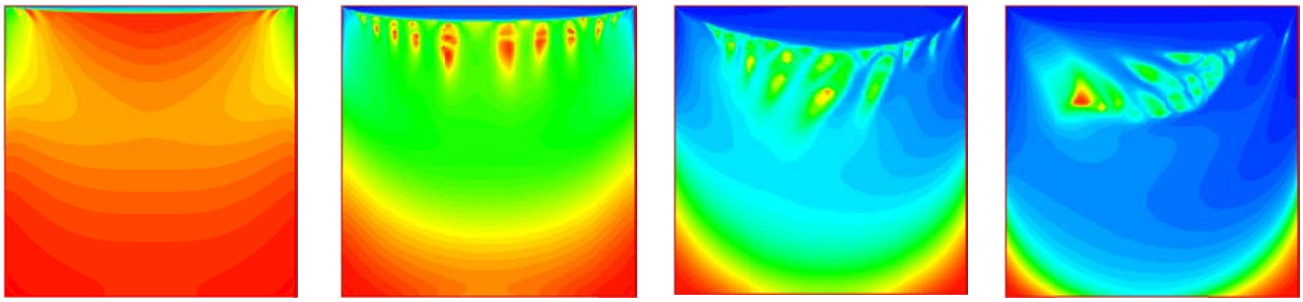
(a) (b) (c) (d)

Fig. 11. Isotherms for φ = 1.0% , for Gr=106 and for (a) Re = 10, (b) Re = 100 , (c) Re = 100 and (d) Re = 2000.



(a) (b) (c) (d)

Fig. 12. shear rate field for φ = 1.0% , for Gr=10^4 and for (a) Re = 10, (b) Re = 100 , (c) Re = 100 and (d) Re = 2000.



(a) (b) (c) (d)

Fig. 13. viscosity field for φ = 1.0% , for Gr=10^4 and for (a) *Re* = 10, (b) *Re* = 100 , (c) *Re* = 100 and (d) *Re* = 2000.

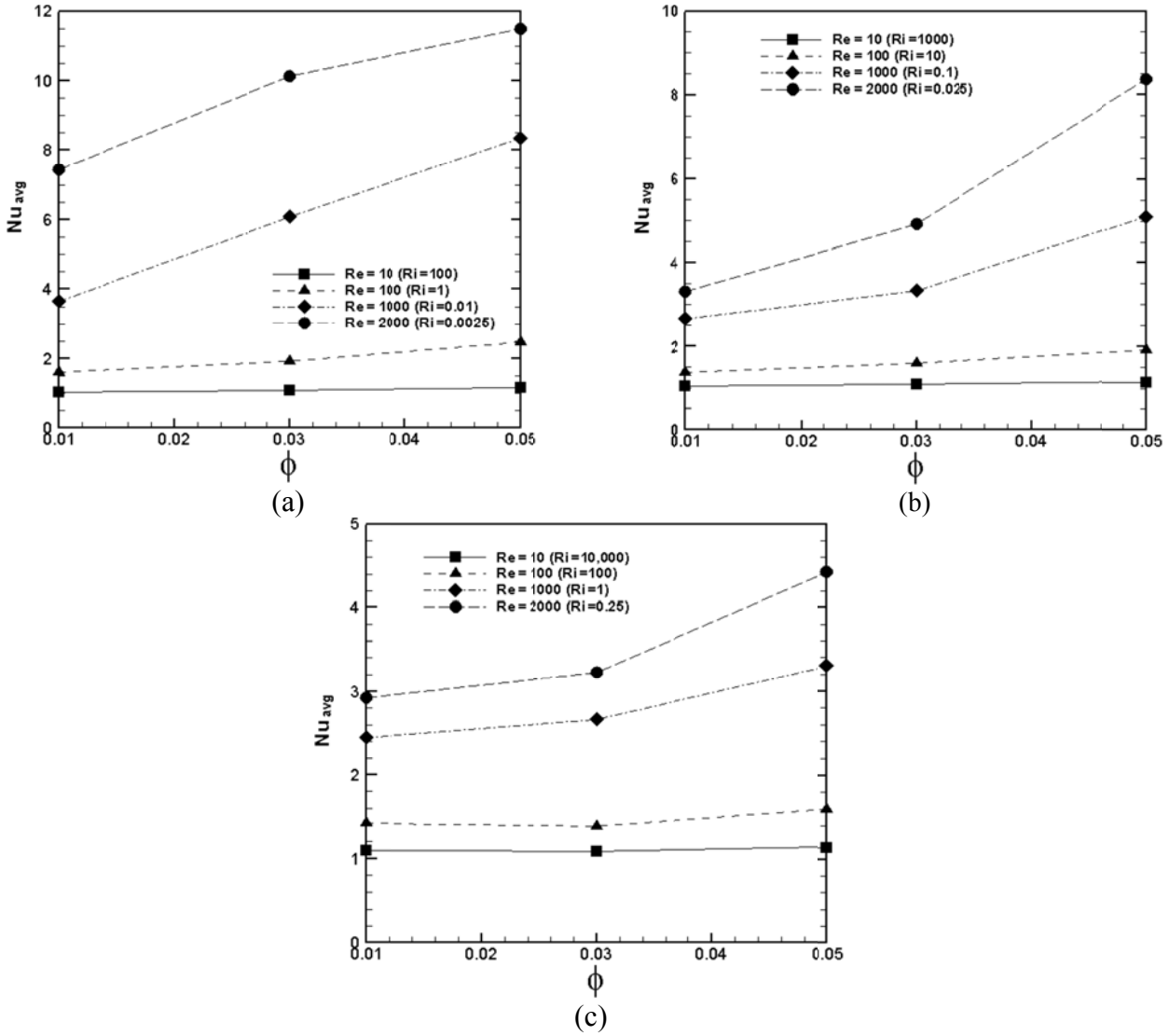


Fig. 14. Variation of average Nusselt number with solid volume fraction for different *Re* (non-Newtonian behavior) (a) *Gr* = 10^4, (b) *Gr* = 10^5, (c) *Gr* = 10^6.

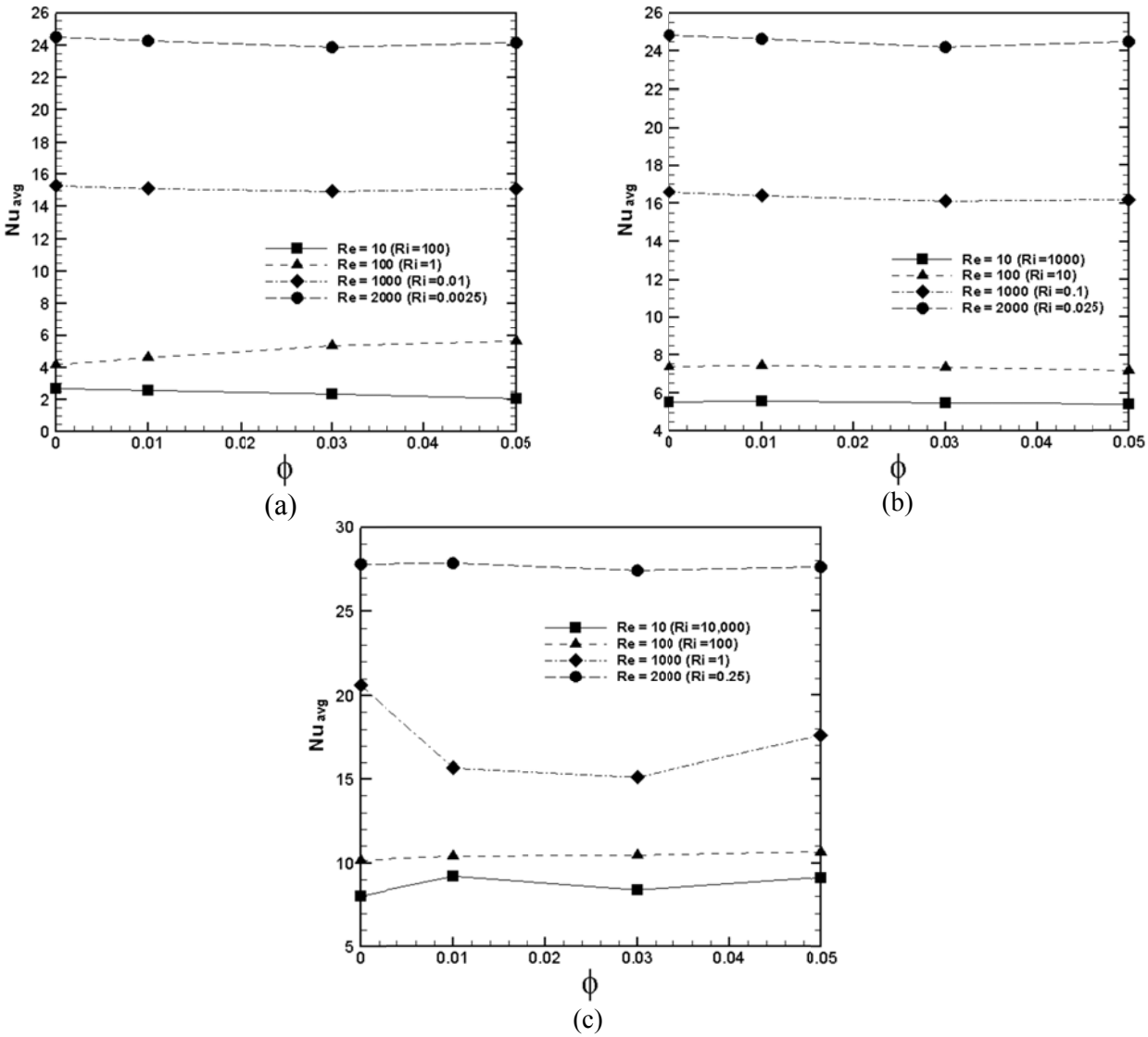


Fig. 15. Variation of average Nusselt number with solid volume fraction for different *Re* (Newtonian behavior) (a) $Gr = 10^4$, (b) $Gr = 10^5$, (c) $Gr = 10^6$.

References

[1] X. Wang, S.U.S. Choi: Thermal conductivity of nanoparticle–fluid mixture, J. of Thermophysics Heat Transfer 13 (1999) 474–480.

[2] J. Chevalier, O. Tillement, F. Ayela: Rheogical properties of nanofluids flowing through microchannels, Appl. Phy. Lett 91 (2007) 233103.

[3] B. Aladag, S. Halelfadl, N. Doner, T. Maré, S. Duret, P. Estellé: Experimental investigations of the viscosity of nanofluids at low temperatures, Appl. Energy 97 (2012) 876–880.

[4] K. Kwak, C. Kim: Viscosity and thermal conductivity of copper oxide nanofluid dispersed in ethylene glycol, Korea–Australia Rheology J 17 (2005) 35–40.

[5] H. Chang, C.S. Jwo, C.H. Lo, T.T. Tsung, M.J. Kao, H.M. Lin, Rheology of CuO nanoparticle suspension prepared by ASNSS, Rev. on Adv. Materials Sci 10 (2005) 128–132.

[6] Y. Ding, H. Alias, D. Wen, R.A. Williams: Heat transfer of aqueous suspensions of carbon nanotubes (CNT nanofluids), Int. J. of Heat and Mass Transfer 49 (2006) 240–250.

[7] J. Hong, D. Kim: Effects of aggregation on the thermal conductivity of alumina/water nanofluids, Thermochimica Acta 542(2012) 28-32.

[8] N. Putra, W. Roetzel, S.K. Das: Natural convection of nano-fluids, Heat and Mass Transfer 39 (2003) 775–784.

[9] D. Wen, Y. Ding, Natural convective heat transfer of suspensions of titanium dioxide nanoparticles (nanofluids), IEEE Transactions on Nanotechnology 5 (2006) 220–227.

[10] A.K. Santra, S. Sen, N. Chakraborty Study of heat transfer augmentation in a differentially heated square cavity using copper–water nanofluid, Int. J. of Therm. Sci 47 (2008) 1113–1122.

[11] M.M. Cross Rheology of non-Newtonian fluids, a new flow equation for pseudoplastic systems, J. of Colloid Sci 20 (1965) 417-437.

[12] H. Ozoe, S. Churchill, Hydrodynamic stability and natural convection in Ostwald-De Waele and Ellis fluids: the development of a numerical solution, AIChE J 18 (1972) 1196-1207.

[13] G.B. Kim, J.M. Hyun, H.S. Kwak, Transient buoyant convection of a power-law non-Newtonian fluid in an enclosure, Int. J. of Heat and Mass Transfer 46 (2003) 3605-3617.

[14] N. Ouertatani, N. Ben Cheikh, B. Ben Beyaa, T. Lilia, T., A. Campo, Mixed convection in a double lid-driven cubic cavity, Int. J. of Therm. Sci 48 (2009) 1265–1272.

[15] R. Iwatsu, J. Hyun, K. Kuwahara, Mixed convection in a driven cavity with a stable vertical temperature gradient, Int. J. of Heat and Mass Transfer 36 (1993) 1601–1608

[16] K. Khanafer, A.J. Chamkha, Mixed convection flow in a lid-driven enclosure filled with a fluid-saturated porous medium, Int. J. of Heat and Mass Transfer 42 (1999) 2465–2481.

[17] O. Aydin, Aiding and opposing mechanisms of mixed convection in a shearand buoyancy-driven cavity, Int. Commun.in Heat and Mass Transfer 26 (1999) 1019–1028.

[18] M.A.R. Sharif, Laminar mixed convection in shallow inclined driven cavities with hot moving lid on top and cooled from bottom, Appl. Therm. Engin 27 (2007) 1036–1042.

[19] K.M. Khanafer, A.M. Al-Amiri, I. Pop, Numerical simulation of unsteady mixed convection in a driven cavity, using an externally excited sliding lid, Eurpean J. of Mechanics B/Fluids 26 (2007) 669–687.

[20] M.M. Abdelkhalek, Mixed convection in a square cavity by a perturbation technique, Computer and Material Sci 42 (2008) 212–219.

[21] M.A. Waheed, Mixed convective heat transfer in rectangular enclosures driven by a continuously moving horizontal plate, Int. J. of Heat and Mass Transfer 52 (2009) 5055–5063.

[22] O. Aydin, W.J. Yang, Mixed convection in cavities with a locally heated lower wall and moving sidewalls, Numerical Heat Transfer 37 (2000) 695–710.

[23] H.F. Oztop, I. Dagtekin, Mixed convection in two sided lid driven differentially heated square cavity, Int. J. of Heat and Mass Transfer 47 (2004) 1761–1769.

[24] W.J. Luo, R.J. Yang,Multiple fluid flow and heat transfer solutions in a two sided lid-driven cavity, Int. J. of Heat and Mass Transfer 50 (2007) 2394–2405.

[25] F. Gurcan, Effect of the Reynolds number on streamline bifurcations in a double-lid-driven cavity with free surfaces, Computer & Fluids 32 (2003) 1283–1298.

[26] R.K. Tiwari, M.K. Das, Heat transfer augmentation in a two-sided lid-driven differentially heated square cavity utilizing nanofluids, Int. J. of Heat and Mass Transfer 50 (2007) 2002–2018.

[27] M. Muthtamilselvan, P. Kandaswamy, J. Lee, Heat transfer enhancement of copper–water nanofluids in a lid-driven enclosure, Commun. in Nonlinear Sci. and Numerical Simulation 15 (2010) 1501–1510.

[28] H.C. Brinkman, The viscosity of concentrated suspensions and solution, J. Chem. Phy 20 (1952) 571–581.

[29] N. Ait Messaoudene, A. Horimek, C. Nouar, B. Benaouda-Zouaoui, Laminar mixed convection in an eccentric annular horizontal duct for a thermodependent non-Newtonian fluid, Int. J. Heat Mass Transfer 54 (2011) 4220-4234.

[30] A. Mahdy, Soret and Dufour effect on double diffusion mixed convection from a vertical surface in a porous medium saturated with a non-Newtonian fluid, J. Non-Newtonian Fluid Mechanics165 (2010) 568-575.

[31] Ahmed M. Salem, Mohamed Abd El-Aziz, Emad M. Abo-Eldahab, Ibrahim Abd-Elfatah, Effect of variable density on hydromagnetic mixed convection flow of a non-Newtonian fluid past a moving vertical plate, Commun. Nonlinear Sci. Num. Simulation 15(6) (2010) 1485-1493

[32] R.B. Bird, W.E. Stewert, E.N. Lightfoot: Transport Phenomena, John Wiley & Sons, Singapore, 1960.

[33] K. Khanafer, K. Vafai, A critical synthesis of thermophysical characteristics of nanofluids, Int. J. of Heat and Mass Transfer 54 (2011) 4410–4428.

[34] A. Barnes, Handbook of Elementary Rheology, Howard University of Wales, Institute of Non-Newtonian Fluid Mechanics, Aberystwyth 2000.

[35] Y. Xuan, W. Roetzel, Conceptions for heat transfer correlation of nanofluids, Int. J. of Heat and Mass Transfer 43 (2000) 3701–3707.

[36] H.E. Patel, T. Sundarrajan, T., Pradeep, A. Dasgupta, N. Dasgupta, S.K. Das, A micro-convection model for thermal conductivity of nanofluid, Pramana J. of Phy 65 (2005) 863–869.

[37] S.V. Patankar, Numerical Heat Transfer and Fluid Flow, Hemisphere, Washington, DC, 1980.

[38] A.J. Chamkha, E. Abu-Nada, Mixed convection flow in single and doublelid driven square cavities filled with water–Al2O3 nanofluid: Effect of viscosity models, European J. Mechanics B/Fluids 36 (2012) 82-96.

[39] S.Z. Heris, S.Gh. Etemad, M.N. Esfahany, Experimental investigation of oxide nanofluids laminar flow convective heat transfer, Int. Commun. in Heat Mass Transfer 33 (2006) 529–535.